Factors Affecting Bond between New and Old Concrete

Article *in* ACI Materials Journal · July 2011

CITATIONS
191

READS
10,636

2 authors:

Pedro M D Santos

33 PUBLICATIONS **1,558** CITATIONS

SEE PROFILE

Eduardo Nuno Brito Santos Júlio

Instituto Superior Técnico

395 PUBLICATIONS **8,396** CITATIONS

SEE PROFILE

ACI MATERIALS JOURNAL TECHNICAL PAPER

Title no. 108-M48

Factors Affecting Bond between New and Old Concrete

by Pedro Miguel Duarte Santos and Eduardo Nuno Brito Santos Júlio

The bond strength of concrete-to-concrete interfaces, of reinforced concrete (RC) members with parts cast at different ages, is highly influenced by the curing conditions. Therefore, the monolithic behavior is dependent on these conditions. Current design codes only consider: a) the concrete compressive strength; b) the normal stress at the interface; c) the amount of reinforcement crossing the interface; and d) the roughness of the substrate surface. Because the curing conditions of both substrate and added concrete are ignored, the influence of the differential shrinkage is neglected. The influence of the differential stiffness due to the mismatch between the Young's modulus of both materials is not considered either.

This paper presents an experimental study conducted to assess the influence of differential shrinkage and stiffness on the bond strength of new-to-old concrete interfaces. Both parameters were shown to have a significant influence on the bond strength and failure mode of concrete-to-concrete interfaces.

Keywords: bond; interface; roughness; shrinkage; stiffness; strength.

INTRODUCTION

The bond strength at the interface between concrete layers cast at different ages is important to ensure the monolithic behavior of reinforced concrete (RC) composite members. Precast beams with cast-in-place slabs and strengthening of existing concrete members by adding a new concrete layer are typical examples of RC composite members.

Current design codes[1-3] present expressions for the assessment of the longitudinal shear strength of the interface between parts of concrete members cast at different ages. These expressions are based on the shear-friction theory, being the longitudinal shear strength evaluated considering the following parameters: a) the compressive strength of the weakest concrete; b) the normal stress at the interface; c) the amount of reinforcement crossing the interface; and d) the roughness of the substrate surface.

These design codes do not take into account the curing conditions of the substrate concrete and of the added concrete layer. This has a significant influence because it can create additional stresses at the interface between both layers due to differential shrinkage. For this reason, the actual design expressions may not be conservative and improvements are needed to increase their accuracy. The differential stiffness due to the difference between Young's modulus is not addressed either.

An experimental study was conducted to assess the influence of the differential shrinkage and differential stiffness between the substrate concrete and the added concrete layer. The adopted materials and methods are presented and the performed tasks are described. Results are presented and discussed. The influence of the adopted bond tests on results is also addressed and failure modes are taken into account in the analysis. An analytical/numerical study was conducted to further analyze the experimental results and discuss both adhesive (interface debonding) and cohesive failures (monolithic failure), and conclusions are made.

RESEARCH SIGNIFICANCE

The bond between concrete parts cast at different ages is affected by several parameters such as the surface preparation method adopted to remove the damaged concrete and to increase the roughness of the substrate. Differential shrinkage and differential stiffness between concrete parts can also have a significant influence on the behavior of the interface. Both parameters are neglected by current design codes. The influence of surface roughness and differential shrinkage and stiffness in the behavior of RC composite members was experimentally investigated. Different curing conditions, surface preparation methods, and interface stress states were considered.

MATERIALS AND METHODS

The materials and methods adopted in the experimental study are described in this section, including the curing conditions, the considered differences of ages between concrete layers, the selected bond tests, the adopted concrete mixture, the instrumentation used to measure the concrete shrinkage, and the techniques adopted to prepare the interface surface and increase its roughness.

Curing conditions

Two curing conditions were considered. One set of concrete specimens was stored in the laboratory and another set was stored outside, directly exposed to the environmental conditions such as solar radiation, rain, and wind. Table 1 presents the average (AVG), standard deviation (STD), and coefficient of variation (COV) of the temperature, as well as relative humidity, which were recorded using a hygrothermograph. Figure 1 presents the variation of temperature and relative humidity during the curing period.

Difference of ages between concrete layers

Three different times were considered for the time gap between casting the substrate and the added concrete layer: 28, 56, and 84 days, with the aim of studying the effect of differential shrinkage between concrete parts. Six sets of specimens were produced: L28, L56, and L84 (L series); and E28, E56, and E84 (E series), where L reports to the specimens cured in the laboratory and E to those cured in the exterior of the laboratory, followed by the difference of age, in days, between casting the substrate and the added concrete layer.

Bond tests

The slant shear test[4] and the splitting test[5] were adopted to assess the bond strength of the interface in shear and in

ACI Materials Journal, V. 108, No. 4, July-August 2011.

Pedro Miguel Duarte Santos *is an Adjunct Professor at the Polytechnic Institute of Leiria, Portugal. He received his PhD in the Department of Civil Engineering from the University of Coimbra, Portugal, in 2009, where he also received his MSc in 2005. His research interests include precasting and strengthening, and repair of reinforced concrete (RC) structures.*

ACI member **Eduardo Nuno Brito Santos Júlio** *is a Professor of structural concrete at the DECivil IST Technical University of Lisbon, Portugal. He is a member of ACI Committee 364, Rehabilitation.*

tension, respectively (Fig. 2). The adopted geometry for the slant shear specimens was a 150 x 150 x 450 mm^3 (5.91 x 5.91 x 17.72 in.^{3}) prism with the shear plane at 30 degrees to the vertical. The geometry defined for the splitting specimens was a 150 mm (5.91 in.) cube with the interface at middle height.

Concrete mixture

The adopted concrete mixture was designed based on the absolute volume expression.[6] A Portland cement Type I 52.5R was adopted to achieve a C50/60 class concrete. Four different aggregates were selected: fine sand, coarse sand, fine limestone crushed aggregates, and coarse limestone crushed aggregates. A commercial admixture was used to increase the hardened concrete initial strength by reducing the water need while retaining the workability of fresh concrete. The maximum dimension of the aggregates was 19.1 mm (0.75 in.), the predicted void volume was 20*l*, and the predicted compacity was 0.822. The reference granulometric curve of Faury was used to determine the proportion of each constituent. The constituents of the adopted concrete mixture are presented in Table 2.

The major goal of this study was to investigate the influence of the differential shrinkage on the bond strength of concrete-to-concrete interfaces. For this reason, one concrete mixture was adopted. Nevertheless, several batches had to be made to produce all specimens and it was observed that differential stiffness has a significant influence on the bond strength and failure mode of the interface. Therefore, it was decided to also include this parameter in the analysis.

The concrete compressive strength[7] on the day of the test of the cubic specimens used for compressive strength control was assessed and the obtained results are presented in Table 3. An average value, corresponding to three concrete specimens, was considered.

Table 1—Temperature and relative humidity

Curing condition/ period	Temperature			Relative humidity		
	AVG, °C (°F)	STD, °C (°F)	COV, %	AVG, %	STD, %	COV, %
Laboratory, from Oct. '06 to Feb. '07	18.2 (64.8)	2.9 (37.2)	15.9	70.3	12.6	17.9
Exterior, from Feb. '07 to May '07	17.5 (63.5)	5.2 (41.4)	29.4	70.8	22.3	31.5

Table 2—Constituents of concrete mixture

Constituent	Diameter range, mm (in.)	Quantity, kg (lb)
Fine sand	0.074 to 9.52 (0.0029 to 0.375)	295 (650)
Coarse sand	0.074 to 9.52 (0.0029 to 0.375)	640 (1421)
Fine limestone	1.19 to 19.1 (0.047 to 0.752)	375 (827)
Coarse limestone	4.76 to 19.1 (0.187 to 0.752)	545 (1202)
Portland cement Type I 52.5R	—	350 (772)
Commercial admixture	—	3.675 (8.102)
Water	—	150 (331)

Shrinkage

Shrinkage was recorded for both curing conditions, using in each case two prismatic 150 x150 x 600 mm^3 (5.91 x 5.91 x 23.62 in.^{3}) specimens.[8] Deformations were measured using, in each specimen, two transducers (Fig. 3). An average value, corresponding to two concrete specimens, was considered. The evolution of the concrete shrinkage with time is presented in Fig. 4.

The experimental shrinkage strain was compared with the theoretical value evaluated according to Eurocode 2.[1] The average compressive strength was 67.3 and 75.8 MPa (9.76 and 10.99 ksi) for specimens cured in the laboratory and in the exterior, respectively. The average relative humidity was 70.3% and 70.8% measured in the laboratory and in the exterior, respectively.

The theoretical predictions of the concrete shrinkage proved to be very conservative. The resemblance between the theoretical predictions, for both curing conditions, is

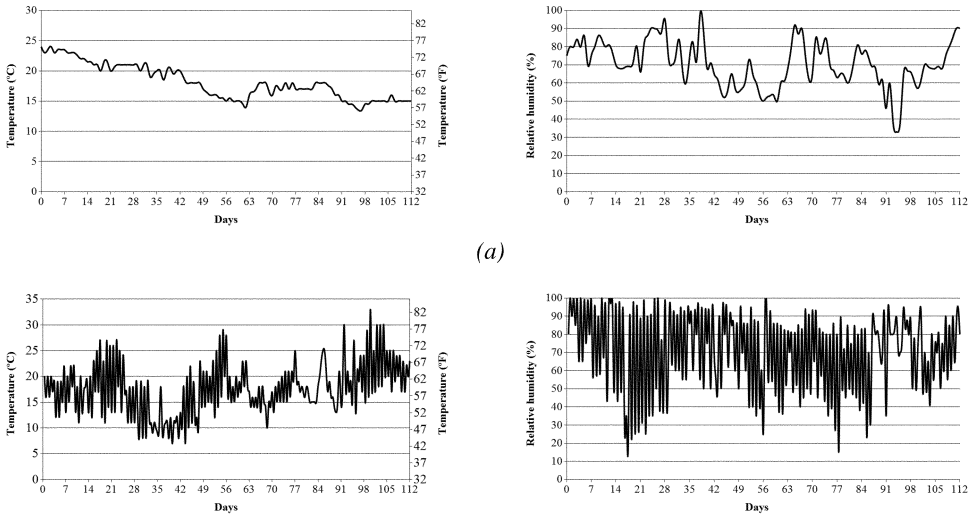

Fig. 1—Temperature and relative humidity: (a) inside laboratory; and (b) outside laboratory.

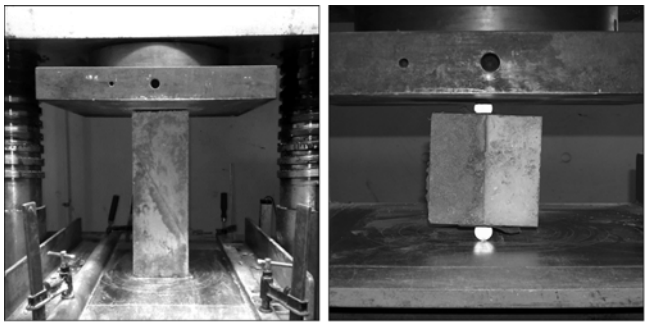

Fig. 2—Bond tests: (a) slant shear test; and (b) splitting test.

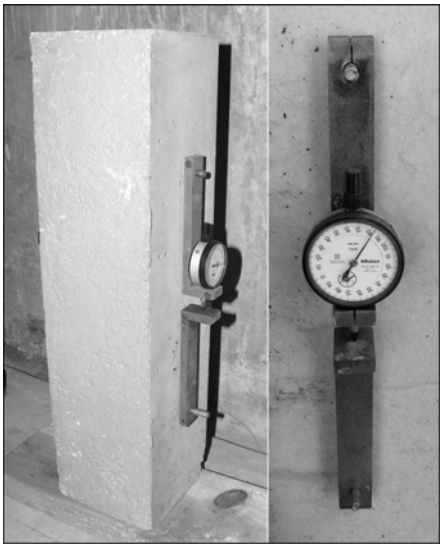

Fig. 3—Concrete specimen for shrinkage measurements.

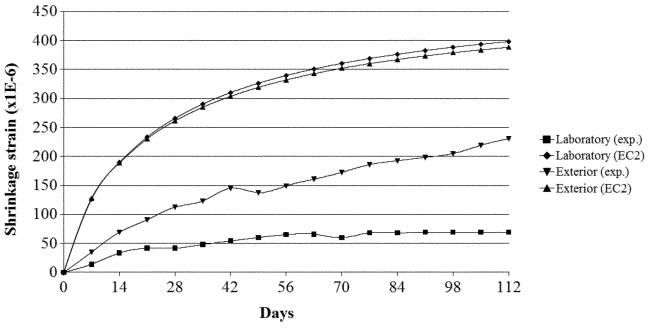

Fig. 4—Evolution of concrete shrinkage strain.

justified taking into account that the average relative humidity is approximately equal in both situations.

The difference between the experimental measurements, for both curing conditions, is explained with the different daily fluctuations of the relative humidity (Table 1). Moreover, the specimens stored outside the laboratory were directly exposed to rain and wind, with respectively a negative and a positive effect in shrinkage increase.

Surface preparation and characterization

Five different situations were considered for the interface surface between the substrate and the added concrete layer (Fig. 5). Left as-cast (LAC) against steel formwork was considered the reference situation. To increase the roughness of hardened concrete, the following treatments were adopted: a) wire-brushing (WB); b) sandblasting (SAB); and c) shotblasting (SHB). Hand-scrubbing (HS), also known as "raking," was adopted to increase the roughness of fresh concrete surfaces. The surface texture was measured with a two-dimensional (2-D) laser roughness analyser,[9] allowing an improved roughness quantification in comparison with other methods.[10] The roughness parameter—maximum valley depth (R_v)—previously identified as the one that best correlates with the bond strength of the interface[9] both in shear and in tension, was adopted.

From each surface type, ten texture profiles were measured and the maximum valley depth (R_v) was computed directly from the primary profile, that is, without filtering.[11] The evaluation length was taken equal to 150 mm (5.91 in.). The assumed values for the maximum valley depth, taken as

Table 3—Compressive strength and age of concrete at test date

Series	Concrete layer	Compressive strength, MPa (ksi)	COV, %	Age at test, days
L28	Substrate	79.3 (11.5)	6.03	56
	Added	66.4 (9.6)	3.18	28
L56	Substrate	86.0 (12.5)	3.50	84
	Added	80.5 (11.7)	1.12	28
L84	Substrate	86.4 (12.5)	2.29	112
	Added	72.6 (10.5)	5.27	28
E28	Substrate	78.9 (11.5)	6.88	56
	Added	68.3 (9.9)	1.05	28
E56	Substrate	77.6 (11.3)	1.98	84
	Added	71.1 (10.3)	5.30	28
E84	Substrate	81.9 (11.9)	0.30	112
	Added	69.9 (10.1)	6.17	28

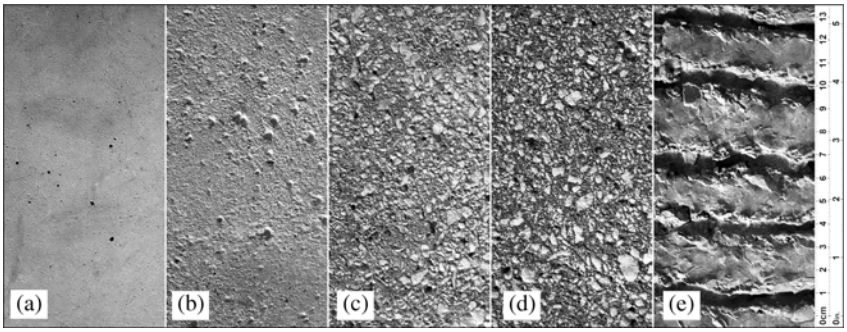

Fig. 5—Surface preparation: (a) left as-cast; (b) wire-brushing; (c) sandblasting; (d) shotblasting; and (e) hand-scrubbing.

Table 4—Maximum valley depth R_v

Surface preparation	Maximum valley depth R_v, mm (in.)
Left as-cast	0.119 (0.005)
Wire-brushing	0.473 (0.019)
Sandblasting	0.604 (0.024)
Shotblasting	0.899 (0.035)
Hand-scrubbing	2.350 (0.093)

Table 5—Experimental results from slant shear and splitting tests

Series	Surface preparation	Slant shear test		Splitting test	
		AVG, MPa (ksi)	COV, %	AVG, MPa (ksi)	COV, %
L28	LAC	10.47 (1.52)	38.31	1.89 (0.27)	11.41
	WB	11.96 (1.74)	15.71	1.78 (0.26)	15.40
	SAB	18.52 (2.69)	25.13	1.98 (0.29)	11.12
	SHB	22.77 (3.30)	14.62	2.35 (0.34)	10.24
	HS	25.39 (3.69)	14.68	3.78 (0.55)	20.50
L56	LAC	10.42 (1.51)	11.66	2.31 (0.34)	17.04
	WB	15.59 (2.26)	21.42	2.14 (0.31)	28.10
	SAB	19.33 (2.81)	24.52	2.14 (0.31)	26.23
	SHB	24.86 (3.61)	4.49	2.40 (0.35)	3.04
	HS	23.39 (3.39)	2.07	3.61 (0.52)	18.70
L84	LAC	19.39 (2.81)	18.15	1.76 (0.26)	2.39
	WB	20.51 (2.98)	9.77	1.86 (0.27)	26.08
	SAB	23.06 (3.35)	6.78	2.38 (0.35)	29.51
	SHB	25.00 (3.63)	4.28	2.32 (0.34)	15.49
	HS	26.86 (3.90)	3.56	3.32 (0.48)	25.14
E28	LAC	8.74 (1.27)	15.39	1.49 (0.22)	23.95
	WB	10.09 (1.46)	28.43	1.68 (0.24)	17.06
	SAB	10.57 (1.53)	15.44	1.67 (0.24)	7.57
	SHB	11.99 (1.74)	23.01	1.89 (0.27)	7.64
	HS	12.45 (1.81)	6.73	2.44 (0.35)	9.27
E56	LAC	10.27 (1.49)	11.32	1.75 (0.25)	26.63
	WB	11.91 (1.73)	20.23	1.82 (0.26)	16.34
	SAB	13.61 (1.98)	10.05	2.28 (0.33)	7.12
	SHB	14.79 (2.15)	8.65	2.35 (0.34)	8.00
	HS	17.73 (2.57)	22.72	2.52 (0.37)	14.23
E84	LAC	13.88 (2.01)	11.04	1.92 (0.28)	8.51
	WB	14.24 (2.07)	20.59	2.03 (0.29)	15.03
	SAB	15.31 (2.22)	28.56	2.27 (0.33)	14.67
	SHB	17.00 (2.47)	18.44	2.46 (0.36)	19.04
	HS	20.79 (3.02)	7.29	2.97 (0.43)	15.48

the average of the values computed from each of the ten profiles, are presented in Table 4.

Cast procedure

For each considered situation—curing condition, surface treatment, and difference of age between concrete layers—five slant shear specimens and five splitting specimens were cast.

First, the substrate concrete was cast. The hand-scrubbed surfaces were prepared while the concrete was still fresh, approximately 2 hours after casting the substrate. All the remaining surface treatments—wire-brushing, sandblasting, and shotblasting—were later executed with hardened concrete. All specimens were kept dry during the curing period except those stored outside the laboratory. All the specimens were dry when the added concrete was placed. After 28, 56, and 84 days, and for each curing condition, the added concrete was cast on the substrate concrete. Before placing back the specimens inside the formwork to cast the added concrete, these were cleaned with compressed air. Two days later, the composite specimens were removed from the formwork and placed again under the considered curing conditions.

When the added concrete reached 28 days of age, the specimens were tested in compression using a standard testing machine. The adopted load rate was 1 kN/s (225 lb/s) for the splitting specimens, 5 kN/s (1124 lb/s) for the slant shear specimens, and 10 kN/s (2248 lb/s) for the cubic specimens for compressive strength control.

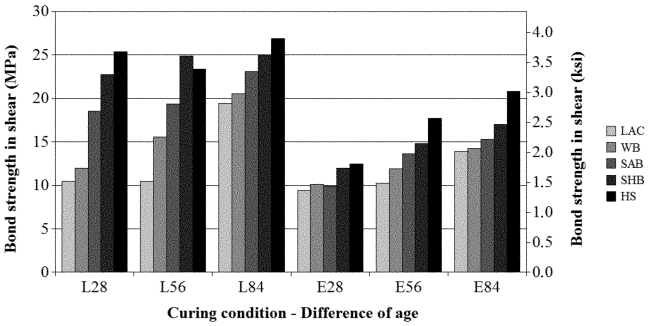

Fig. 6—Bond strength in shear.

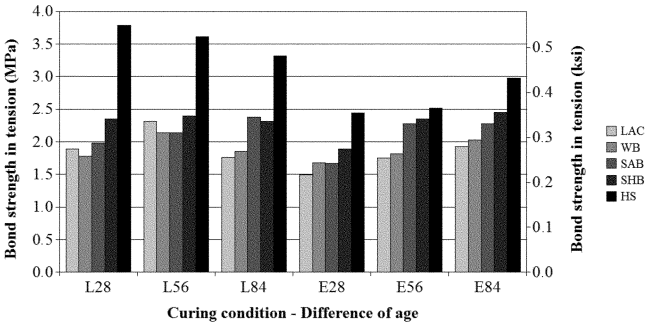

Fig. 7—Bond strength in tension.

EXPERIMENTAL RESULTS

The bond strength in shear was assessed with the slant shear test.[4] An average value, corresponding to five tests, was considered. Shown in Table 5 are the average (AVG) and the coefficient of variation (COV) of the slant shear specimens. Figure 6 presents a comparison of the bond strength of the interface in shear for the L and E series.

The bond strength in tension was assessed with the splitting test.[5] An average value, corresponding to five tests, was considered. In Table 5, the average (AVG) and the coefficient of variation (COV) of the splitting specimens are presented. In Fig. 7, a comparison between the bond strength of the interface in tension for the L and E series is presented.

In general, the bond strength of the interface increased with the increase of the surface roughness, as expected. Nevertheless, an increase of the bond strength with the increase of the difference of ages between the substrate concrete and the added concrete layer was observed, contrary to what was expected.

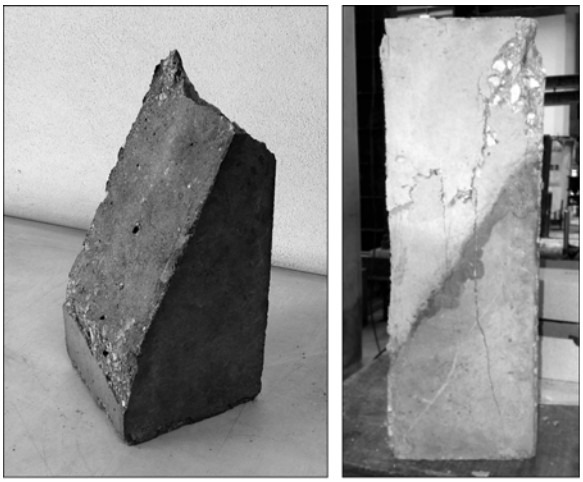

Fig. 8—Failure modes for slant shear test: (a) adhesive; and (b) cohesive.

The increase of the difference of ages implies an increase of the differential shrinkage between concrete layers and, therefore, an increase of stresses at the interface. For this reason, a decrease of the bond strength of the interface was expected, but did not occur.

The assessment of the bond strength in tension proved to be inconclusive. The evolution of the bond strength, with the increase of the surface roughness and with the increase of the difference of ages between concrete layers, is not clear. When comparing the results obtained with the slant shear test with the results achieved with the splitting test, it appears that the latter bond test is unsuitable for this purpose.

Two distinctive failure modes were observed: adhesive (interface debonding) and cohesive (monolithic). Adhesive failure occurs at the interface whenever the bonding strength is reached; cohesive failure occurs in the bulk by concrete crushing. The slant shear specimens presented both failure modes (Fig. 8). The number of cohesive failures in shear is presented in Fig. 9. All splitting specimens presented adhesive failures.

At the interface of specimens presenting adhesive failures, small particles of the overlay were observed, due to mechanical interlock. For specimens presenting cohesive failures, concrete crushing at the overlay (the weakest concrete) was registered.

ANALYTICAL APPROACH

The results obtained with the tested concrete specimens cannot be directly compared because differences between concrete strengths were measured. Moreover, the tested slant shear specimens exhibited both adhesive and cohesive failures. Therefore, the Mohr-Coulomb criterion was adopted to determine the pure shear strength for all specimens and the results analysis was performed based on this parameter. The failure envelopes of both substrate concrete and added concrete were defined using the experimental value of the compressive strength, obtained with three cubic specimens at test date, and the analytical tensile strength was predicted according to Eurocode 2.[1] The failure envelope of the interface was defined using the experimental values of the bond strength in shear and in tension, assessed using the slant shear test and the splitting test, respectively. The failure stress in compression, obtained for the specimens presenting a cohesive failure, was also used to define the failure envelope of these specimens. The pure shear strength was taken as the

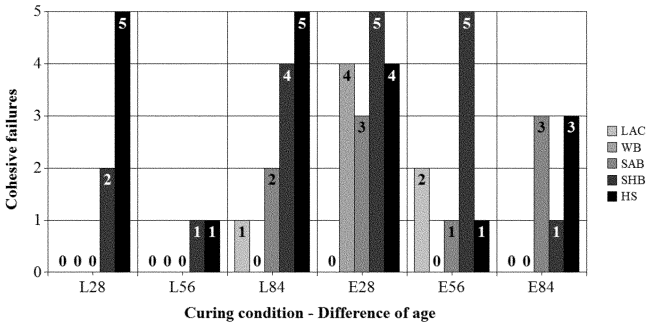

Fig. 9—Number of monolithic failures in shear.

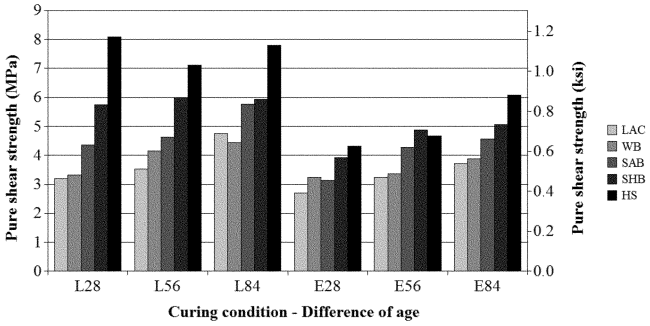

Fig. 10—Pure shear strength.

average of the values corresponding to adhesive and cohesive failures. Figure 10 presents the pure shear strength of the interface for the L and E series.

Surface roughness

From Fig. 10 it can be observed that the pure shear strength of the interface increases, for both curing conditions, with the increase of the surface roughness. Three exceptions were identified for the wire-brushed surface (L84 series), the sandblasted surface (E28 series), and the hand-scrubbed surface (E56 series).

Difference of ages

From Fig. 10 it can be observed that the pure shear strength increases, for both curing conditions, with the increase of the difference of ages between the substrate concrete and the added concrete layer. Three exceptions were identified for the L series, one for the shotblasted surface and two for the hand-scrubbed surface.

This result was not expected because the bond strength of the interface is supposed to decrease with the increase of differential shrinkage, which increases with the difference of ages between concrete layers. For this reason, a numerical study, described below, was conducted to further investigate this matter.

The curing in the exterior led, as expected, to lower values of the pure shear strength, with an average decrease of 1.12 MPa (0.16 ksi), to which corresponds a decrease of 19%.

Failure mode

For the slant shear specimens, the number of cohesive failures (Fig. 9) increased with the increase of the surface roughness of the interface, presenting 3, 4, 9, 18, and 19 failures for the left as-cast, wire-brushed, sandblasted, shotblasted, and hand-scrubbed surfaces, respectively.

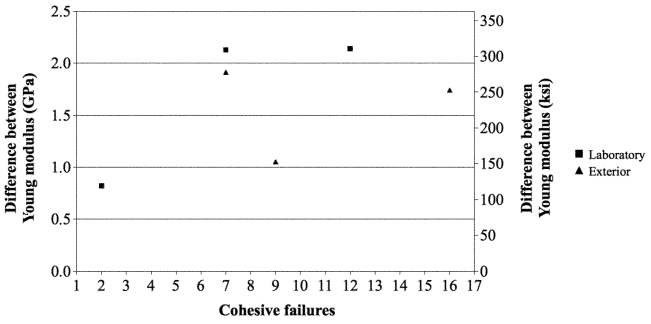

Fig. 11—Differential stiffness versus cohesive failures.

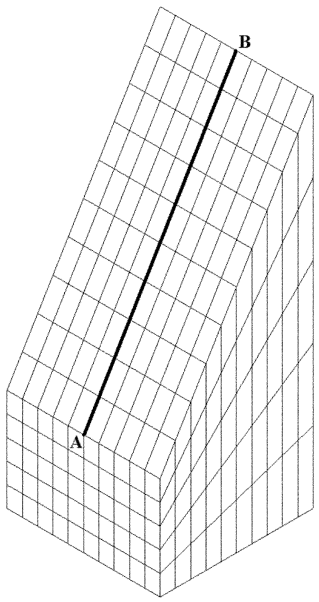

Fig. 12—Finite elements mesh.

Differential stiffness

The concrete specimens were cast in six batches using the same concrete mixture. Nevertheless, different values were obtained for the compressive strength at the test date. These differences, although small, have an influence on the Young's modulus of each concrete layer and, consequently, on the differential stiffness of the composite concrete member.

Several researchers[6,12] stated that the increase of the differential stiffness between concrete layers changes the stress distribution at the interface, and stress concentrations are observed at both ends.

Several slant shear specimens exhibited broken corners (Fig. 8(a)). The justification for this phenomenon can be related with the stress distribution at the interface. In fact, these broken corners are located precisely at both ends of the interface.

Despite the reduced number of concrete specimens, an increase in the number of cohesive failures with the increase of the difference between the Young's modulus of both concrete layers was observed (Fig. 11), corroborating the results of previous studies.[6]

The existence of a correlation between these two parameters—cohesive failure and differential stiffness—is extremely important because it means that it is possible to change the failure mode of a composite concrete member by designing the differential stiffness between both concrete layers.

NUMERICAL MODELING

To understand the influence of differential shrinkage and differential stiffness on the bond strength of the interface, a numerical study was conducted using commercial finite elements software. First, both parameters were independently considered and, afterward, their effects were superimposed.

A three-dimensional (3-D) model of the slant shear specimen adopted in the experimental study was built using a finite elements mesh with 20-node hexahedrons. A sliced 3-D model of the specimen, with the location of the mean line of the interface (Segment AB), is presented in Fig. 12. Linear material behavior was assumed. Only the nodal displacements at the top and bottom faces were restrained.

Differential shrinkage

To study the effect of differential shrinkage on the stress distribution at the interface, for the considered ages, the experimental shrinkage strain was applied to each half of the concrete specimens, and other relevant material properties were also defined according to the experimental results.

The Young's modulus of the substrate concrete and of the added concrete was assumed according to Eurocode 2,[1] using the values obtained for the compressive concrete strength at the test date. The coefficient of Poisson was considered equal to 0.2.

For the shrinkage strain of the substrate concrete cured under laboratory conditions, the values of 65.0×10^{-6}, 68.3×10^{-6}, and 69.2×10^{-6} for a difference of age between both concrete layers of 28, 56, and 84 days, respectively, were adopted. For the shrinkage strain of the substrate concrete cured in the exterior, the corresponding values of 149.2×10^{-6}, 192.5×10^{-6}, and 230.8×10^{-6}, respectively, were adopted. The shrinkage strain of the added concrete was considered equal to 47.1×10^{-6} and 112.5×10^{-6}, at the age of 28 days, for curing under laboratory conditions and curing in the exterior, respectively.

Figures 13 and 14 present the stress distributions, along the mean line of the interface, for shear and normal stresses, respectively. At the corners of the interface, the average increase of the normal stress in relation to the considered mean line is 62%, varying between 59% and 64%.

As expected, stresses increase with the increase of the differential shrinkage between concrete layers.

Differential stiffness

To study the effect of differential stiffness on the stress distribution at the interface, one strength class was adopted for the substrate concrete and four strength classes were adopted for the added concrete. The material properties were defined according to Eurocode 2.[1] For the substrate concrete, C20/25 class was adopted and, for the added concrete, the following strength classes were considered: C20/25, C25/30, C40/50, and C90/105. The Young's modulus was determined according to Eurocode 2[1]: 30, 31, 35, and 44 GPa (4351, 4496, 5076, and 6382 ksi), respectively. The coefficient of Poisson was considered equal to 0.2.

The nodal displacements at the top and bottom faces were restrained to simulate the effect of friction between the testing machine plates and the concrete specimens. A vertical unit displacement was applied to the bottom face of the model to simulate the action of the testing machine. The distribution of shear and normal stresses, along the mean line of the interface, is presented in Fig. 15 and 16, respectively.

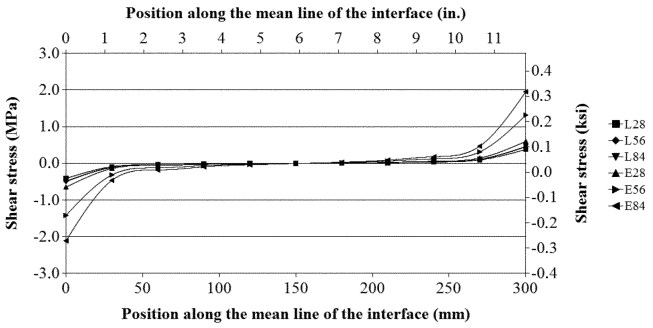

Fig. 13—Shear stress distribution at interface due to differential shrinkage.

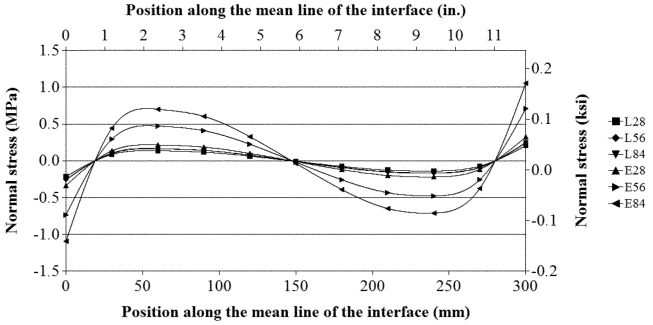

Fig. 14—Normal stress distribution at interface due to differential shrinkage.

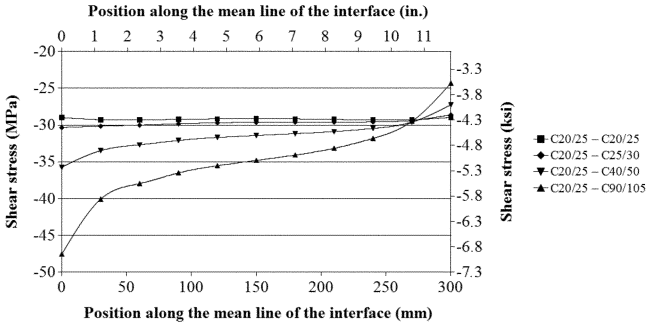

Fig. 15—Shear stress distribution at interface due to differential stiffness.

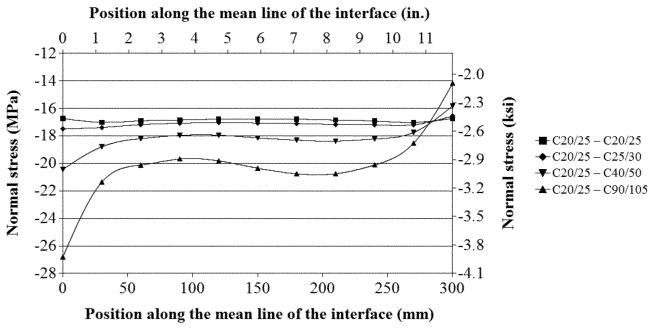

Fig. 16—Normal stress distribution at interface due to differential stiffness.

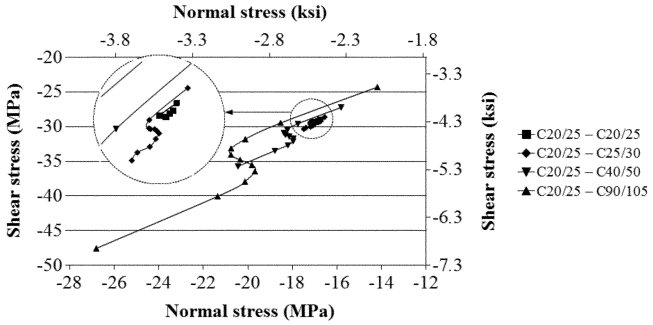

Fig. 17—Comparison of normal stress versus shear stress in interface.

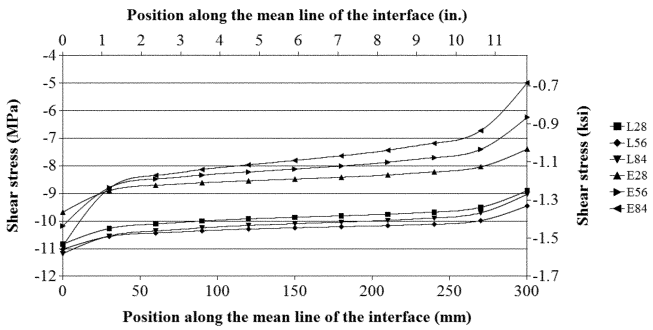

Fig. 18—Shear stress distribution at interface.

The stress distribution at the interface, for both shear and normal stresses, is influenced by the differential stiffness. With the increase of the differential stiffness, stress concentrations occur at both ends and the stress distribution assumes an S-shaped form.

Analyzing the evolution of the normal stress with the shear stress, it is possible to conclude that for the same level of the latter, the corresponding normal stress increases with the increase of the differential stiffness between concrete parts (Fig. 17). This conclusion can be reached plotting a horizontal line in the graph of Fig. 17 to intersect the S-shaped lines. This type of evolution can explain the different failure modes observed for the slant shear specimens because the normal compressive stresses increase, for the same shear stress, with the differential stiffness.

Combined effect of differential shrinkage and differential stiffness

The material and time-dependent properties of concretes used in the experimental study were adopted in the 3-D model to perform the analysis of the combined effect of differential shrinkage and differential stiffness with the compressive loading at the test date.

The vertical displacement imposed to simulate the compression of the testing machine was taken equal to 40% of the average compressive strength of a C50/60 strength class. This value was adopted because it is used, as suggested by Eurocode 2,[1] for the determination of the secant modulus of elasticity of concrete.

The distribution of shear, normal, and equivalent stresses (von Mises stress), along the mean line of the interface, is presented in Fig. 18 to 20, respectively.

At the test date, the concrete specimens were already subjected to a stress state due to differential shrinkage. With compressive loading, tension stresses due to differential shrinkage disappear from the interface. The combined effect of the differential shrinkage, differential stiffness, and compressive loading during testing revealed that the failure load increases with the difference of ages between concrete layers and, thus, with the differential shrinkage, which was

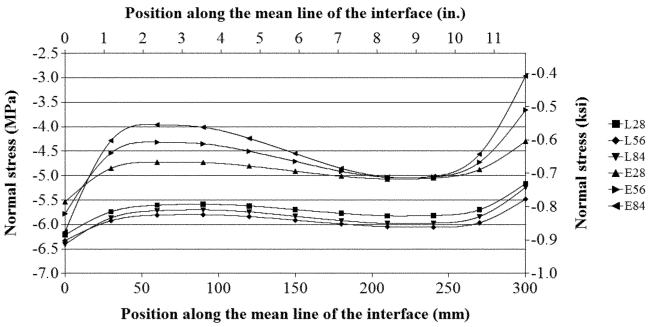

Fig. 19—Normal stress distribution at interface.

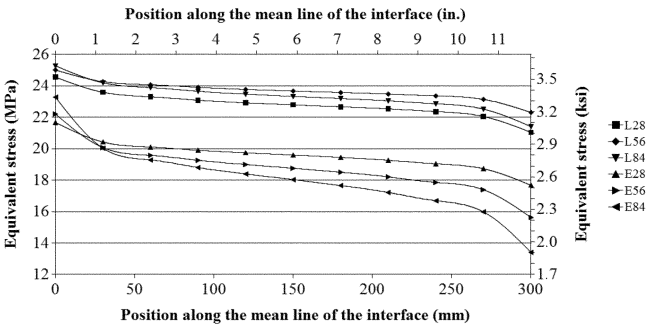

Fig. 20—Equivalent stress distribution at interface.

contrary to what was first expected. This can be observed in Fig. 18 to 20, with the only exception being the L28 series. It should be added that comparisons between L and E series, for the same difference of ages, cannot be made because other influencing parameters, besides shrinkage, are also present but were not assessed.

CONCLUSIONS

For both curing conditions, inside and outside the laboratory, the average values of temperature and relative humidity were very similar, whereas the coefficient of variation for the first situation was approximately the double relative to the second, due to higher daily fluctuations of both parameters.

The prediction of shrinkage by Eurocode 2[1] was shown to be very conservative. The experimental measurements for both curing conditions were considerably different, mainly due to daily fluctuations of the relative humidity and temperature and also to the direct exposure of the concrete specimens to rain and wind outside the laboratory.

The slant shear test appeared to be suitable to predict both the bond strength and the failure mode of the interface. The modified splitting test appears to be unsuitable for both purposes. Further research is needed to investigate the assessment of the bond strength using the splitting test.

The bond strength of the concrete-to-concrete interface increased with the increase of the surface roughness. Comparing both curing conditions, a significant decrease of the bond strength was observed from the curing in the laboratory to the curing in exterior conditions. The average decrease of the bond strength was 19%.

The developed numerical model showed that the differential stiffness could have influence in the bond strength of the interface. The failure mode is also influenced because the failure mode can change from adhesive to cohesive.

The bond strength of the concrete-to-concrete interface increased with the increase of the difference of age between concrete layers. This result was not expected and a numerical simulation was performed to justify it. The numerical model corroborated the experimental observations because the compressive loading eliminates the tension stresses at the interface of slant shear specimens, due to the differential shrinkage. Therefore, with the increase of the difference of age between concrete layers, corresponding to a higher differential shrinkage, the failure load of the slant shear specimens also increases. This beneficial effect should be verified for other structural concrete-to-concrete interfaces, and thus to other stress states.

The influence of Young's modulus of each concrete layer should be investigated in future research.

This research study proved that both differential shrinkage and differential stiffness can have a significant influence on the behavior of concrete-to-concrete interfaces, namely on the bond strength and failure mode. Therefore, it can be stated that the design expressions of current design codes should be improved to incorporate the consideration of these parameters, thus increasing their accuracy.

ACKNOWLEDGMENTS

This research project has been funded by the Portuguese Science and Technology Foundation (FCT) with reference PTDC/ECM/098497/2008. Acknowledgements are extended to MAPREL – Empresa de Pavimentos e Materiais Pré-Esforçados Lda, SIKA Portugal SA, AFAssociados – Projectos de Engenharia SA, WEBER Cimenfix, CIMPOR – Cimentos de Portugal, BETÃO-LIZ Adémia, and Euro-Planning – Engenharia & Gestão Lda for their financial and material support.

REFERENCES

1. EN 1992-1-1, "Eurocode 2—Design of Concrete Structures—Part 1: General Rules and Rules for Buildings," European Committee for Standardization, Brussels, Belgium, 2004, 225 pp.

2. ACI Committee 318, "Building Code Requirements for Structural Concrete (ACI 318M-08) and Commentary," American Concrete Institute, Farmington Hills, MI, 2008, 473 pp.

3. CAN/CSA-A23.3-04, "Design of Concrete Structures—Structures Design," Canadian Standards Association, Rexdale, ON, Canada, 2004, 258 pp.

4. EN 12615, "Products and Systems for the Protection and Repair of Concrete Structures—Test Methods—Determination of Slant Shear Strength," European Committee for Standardization, Brussels, Belgium, 1999, 12 pp.

5. EN 12390-6, "Testing Hardened Concrete—Part 6: Tensile Splitting Strength of Test Specimens," European Committee for Standardization, Brussels, Belgium, 2004, 14 pp.

6. Júlio, E. N. B. S.; Branco, F. A.; Silva, V. D.; and Lourenço, J. F., "Influence of Added Concrete Compressive Strength on Adhesion to an Existing Concrete Substrate," *Build and Environment*, V. 41, No. 12, Dec. 2006, pp. 1934-1939.

7. EN 12390-3, "Testing Hardened Concrete—Part 3: Compressive Strength of Test Specimens," European Committee for Standardization, Brussels, Belgium, 2003, 21 pp.

8. LNEC E 398, "Concrete—Determination of Shrinkage and Expansion," LNEC, 1993, 2 pp. (in Portuguese)

9. Santos, P.; and Júlio, E., "Development of a Laser Roughness Analyser to Predict In-Situ the Bond Strength of Concrete-to-Concrete Interfaces," *Magazine of Concrete Research*, V. 60, No. 5, June 2008, pp. 329-337.

10. Santos, P. M. D.; and Júlio, E. N. B. S., "Comparison of Methods for Texture Assessment of Concrete Surfaces," *ACI Materials Journal*, V. 107, No. 5, Sept.-Oct. 2010, pp. 433-440.

11. Santos, P. M. D.; and Júlio, E. N. B. S., "Effect of Filtering on Texture Assessment of Concrete Surfaces," *ACI Materials Journal*, V. 107, No. 1, Jan.-Feb. 2010, pp. 31-36.

12. Austin, S.; Robins, P.; and Pan, Y., "Shear Bond Testing of Concrete Repairs," *Cement and Concrete Research*, V. 29, No. 7, July 1999, pp. 1067-1076.